A Hybrid Self-Optimizing Simulated Annealing and Particle Swarm Optimization Approach for PMSM Parameter Optimization

Zhenyu Luo[1*], Hexiong Chen[1], Shuang He[2], Qian Zhang[3]
[1]Information Center of Yunnan Power Grid Co., Ltd., Kunming, 650011, China
[2]Honghe Power Supply Bureau of Yunnan Power Grid Co., Ltd., Kunming, 661000, China
[3]Kunming Power Supply Bureau of Yunnan Power Grid Co., Ltd., Kunming, 650011, China
E-mail: Luo_ZhenyuRTM@outlook.com
[*]Corresponding author

Keywords: PMSM, SA, PSO, parameter optimization, greedy optimization strategy

Received: September 20, 2024

In the power system, permanent magnet synchronous motors are an important component of the key assets in power grid companies. To improve the operational efficiency of permanent magnet synchronous motors and reduce maintenance costs, a parameter optimization method combining self-optimizing Simulated Annealing (SA) and Particle Swarm Optimization (PSO) is designed. This method utilizes the powerful global search performance of SA to avoid local optimal solutions, and combines the fast convergence characteristics of PSO to achieve precise and efficient parameter tuning. At the same time, greedy optimization strategy and memory tempering mechanism are introduced into the PSO. A self-optimizing strategy based on SA and PSO is designed. The specific method used in the study is to combine the powerful global search ability of SA algorithm with the fast convergence characteristics of PSO algorithm, integrate the advantages of both algorithms, and achieve fast and accurate identification of motor parameters. By incorporating greedy optimization strategies and memory tempering mechanisms within the PSO framework, the limitations of insufficient accuracy in handling multivariate parameter identification problems can be addressed. From the results, the parameters of the permanent magnet synchronous motor optimized by the self-optimizing resulted in a direct axis inductance error of 0.62%, a quadrature axis inductance error of 0.31%, a resistance error of 0.34%, and a magnetic linkage error of 5.14%. In addition, the standard deviation of the self-optimizing SA-PSO was 0.04, which was 0.15, 0.10, and 0.06 lower than the standard deviations of PSO, SA, and SA-PSO algorithms of 0.19, 0.14, and 0.10, respectively. In terms of stability, the standard deviation of the hybrid strategy was 0.012, which was 73.33%, 69.23%, and 57.14% lower than PSO, SA, and traditional SA-PSO, respectively. Therefore, the permanent magnet synchronous motor parameter system optimized by combining self-optimizing SA with PSO effectively reduces energy consumption during operation, which helps the power grid company to achieve dual benefits in economic benefits and environmental sustainability.

Povzetek: Študija predstavlja hibridni pristop optimizacije parametrov PMSM, ki združuje samooptimizacijsko simulirano kaljenje (SA) in optimizacijo rojev delcev (PSO). Metoda izkorišča globalne iskalne sposobnosti SA in hitro konvergenco PSO. Z vključitvijo strategije požrešne optimizacije in mehanizma temperaturnega popuščanja v PSO, hibridni algoritem dosega boljšo identifikacijo parametrov motorja, kar zmanjšuje porabo energije in prispeva k ekonomskim in okoljskim koristim.

1 Introduction

Permanent Magnet Synchronous Motor (PMSM), as a key component in modern power systems, its parameter stability directly affects the high-performance of control systems. The parameter changes of the motor during operation may lead to a decrease in control performance, which is particularly unfavorable for application scenarios that pursue high-precision control [1-2]. In traditional control theory, sliding mode variable structure control and adaptive control have improved the robustness of the system to a certain extent. However, these methods cannot fundamentally eliminate the impact of parameter changes on the controller, and instead increase the complexity of controller [3]. Faced with this challenge, directly identifying motor parameters has become a key way to solve the problem, which not only helps to improve control performance, but also serves as the foundation for achieving motor health status monitoring [4]. However, quickly and accurately obtaining the motor parameters under different operating conditions has always been a challenge in control theory and practice [5]. Therefore, exploring efficient methods to identify motor parameters has important theoretical and practical value for optimizing motor control systems. In this context, a hybrid optimization strategy is proposed by combining self-optimizing Simulated Annealing (SA) and Particle

Swarm Optimization (PSO) to optimize the parameter identification process of PMSM. This method aims to integrate the advantages of two algorithms, combining the strong global search performance of SA with the fast convergence characteristics of PSO to quickly and accurately identify motor parameters. This study innovatively develops an optimization method that can adapt to changes in motor parameters and improve system robustness, aiming to provide support for the design and implementation of high-precision motor control systems, and enhance the stability and efficiency of power systems. The research content mainly includes four parts. The first part is the background of PMSM. The second part reviews the research status of PMSM and PSO both domestically and internationally. The third part designs a hybrid optimization strategy for PMSM parameters based on self-optimizing SA algorithm and PSO. The first section conducts parameter design for PMSM based on PSO optimization. The second section designs a PMSM parameter system optimized by combining self-optimizing SA with PSO. The fourth part verifies the PMSM parameter hybrid optimization strategy based on self-optimizing SA and PSO.

2 Related works

PMSM has been widely used in high-performance control systems due to its simple structure and high stability. Therefore, it has become a research focus, giving rise to a large number of research results. Sun X et al. designed a PMSM to meet specific campus patrol electric vehicle driving needs. A method for adjusting the structure of permanent magnets was proposed. The results showed that this method reduced torque ripple by 24% [6]. To design an efficient surface PMSM, He C et al. built an analysis method based on a finite element model, which selected a lower torque angle to enhance the overload capacity of the motor. The results showed that this method achieved efficient motor performance [7]. Palangar M F et al. used multi-objective optimization methods to improve the performance of PMSM in transient and steady-state performance. It improved the overall performance of PMSM [8].

The PSO significantly contributes to optimizing the performance of PMSM. To overcome the tendency of traditional PSO to lose diversity and fall into local optima during the iteration process, Zaman H R R et al. proposed an enhanced PSO that integrated backtracking search optimization algorithm. The algorithm introduced a neighborhood modification mechanism based on backtracking search optimization algorithm. The results showed that this method was effective [9]. Liu W et al. built a novel adaptive weighted PSO to improve the search ability of the PSO. It adaptively adjusted the acceleration coefficient by developing a weighting strategy based on the Sigmoid function. The results showed that the algorithm had excellent search ability [10]. Luo X et al. proposed a position transition PSO to overcome the premature convergence in latent factor analysis models. This algorithm optimized high-dimensional sparse matrices through a population strategy with adaptive learning rates. The results showed that this method achieved higher prediction accuracy when dealing with missing data [11]. The method summary table is shown in Table 1.

In summary, significant progress has been made in research on PMSM and PSO. However, the combination of self-optimizing SA and PSO parameter optimization method to optimize the design parameters of PMSM is still relatively rare in existing research. To this end, an innovative hybrid optimization strategy is proposed, which effectively integrates the global search of the SA with the fast convergence characteristics of the PSO. Based on this hybrid method, the aim is to achieve fast and accurate motor parameter identification, improving the efficiency of parameter design and the optimization performance of motor performance.

Table 1. Method summary

Method	Author	Result	Limitations
Method for adjusting the structure of permanent magnets, air gap length, and stator core geometry	Sun X et al. [6]	The torque ripple has been reduced by 24%	The application environment is limited to the driving requirements of patrol electric vehicles on specific campuses
Analysis method based on finite element model	He C et al. [7]	Achieved efficient motor performance	Mainly optimizing overload capacity, but not fully covering other performance indicators
Multi-objective optimization method	Palangar M Fet al. [8]	Improved the overall performance of permanent magnet synchronous motors	Stability requires more detailed data support
Improved PSO algorithm incorporating backtracking search optimization algorithm	Zaman H R R et al [9].	Improved effectiveness, overcoming the local optimum problem of traditional PSO	Algorithm complexity increases and computation time becomes longer
Adaptive weighted PSO algorithm	Liu W et al [10].	Excellent search capability	Unable to handle high-dimensional

based on sigmoid function weighting strategy Position Transition PSO Algorithm Based on Adaptive Learning Rate Group Strategy	Luo X et al [11].	Achieved higher prediction accuracy when handling missing data	optimization problems Mainly targeting high-dimensional sparse matrices, with limited generality

3 Hybrid optimization strategy for PMSM parameters based on self-optimizing SA and PSO

This chapter explores a hybrid optimization strategy combining SA and PSO, aiming to improve the accuracy and efficiency of parameter design for PMSM. This strategy combines the global search performance of the SA with the fast convergence characteristics of the PSO to finely adjust the motor parameters.

3.1 PMSM parameter design based on PSO algorithm optimization

The PSO mimics the foraging behavior of bird populations [12]. In PSO, solutions are viewed as "particles" moving within the search space, with each particle in the population moving towards the currently determined optimal solution to search for a more optimal solution [13]. However, PSO faces several challenges. Firstly, due to its probabilistic nature, PSO cannot guarantee finding the global optimal solution within limited iterations. The speed and position updates of particles have randomness, which increases the uncertainty in finding the global optimal solution. Secondly, the accuracy is influenced by multiple parameters, including population size, iterations, initial position, inertia weight, and learning factor. Although larger populations and iterations theoretically add the probability of finding the global optimal solution, they also prolong the running time. However, initial position selection and parameter setting often rely on experience, making it difficult to achieve optimal results. Finally, as the iteration progresses, particles tend to aggregate in the search space and fall into local optima, which limits the algorithm's ability to explore later [14]. Given these challenges, this research aims to determine the optimal initial parameters to enhance the convergence speed and optimization accuracy. The PSO flow after initial parameter optimization is shown in Figure 1.

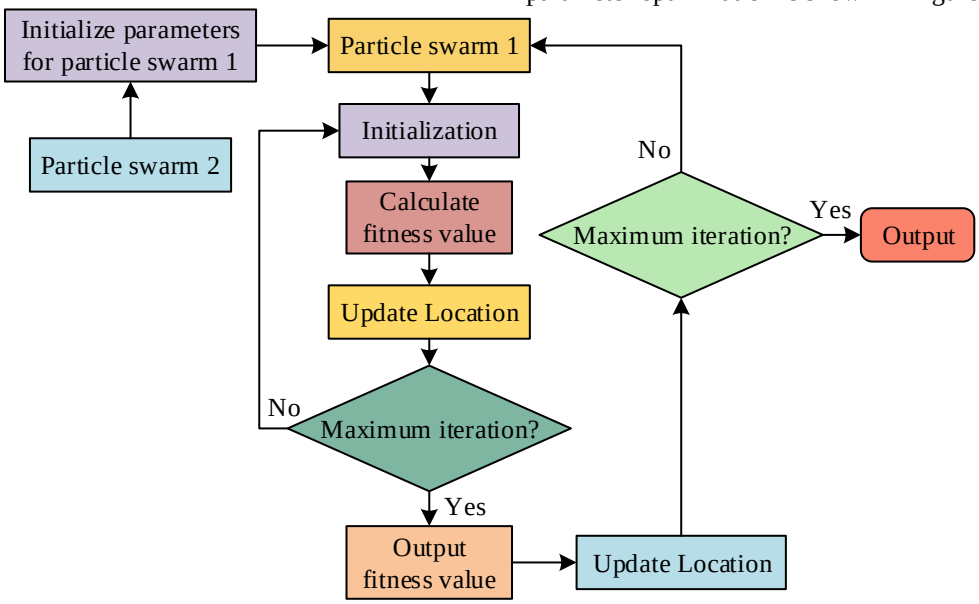

Figure 1: PSO process optimized by initial parameters

In Figure 1, there are two key particle swarms in the initial parameter optimization process of PSO: particle swarms 1 and 2. Particle swarm 1 is the main optimization group, while particle swarm 2 focuses on optimizing the initial parameters of particle swarm 1. Each particle in particle swarm 2 represents a set of initial parameters that may be used for particle swarm 1. These parameters include inertia weight ω, individual learning factor $c1$, and social learning factor $c2$. Particle swarm 1 receives these parameters and evaluates their effectiveness using a fitness function. The fitness value reflects the parameter effectiveness and provides feedback to particle swarm 2. Based on the update rules of position and velocity, particle swarm 2 adjusts its parameters with the goal of finding the optimal parameter combination that minimizes the fitness value of particle swarm 1. Through repeated iterations, particle swarm 2 gradually optimizes parameter selection until reaching the preset maximum iterations. Ultimately, the output parameter set is the

initial parameter configuration that can achieve optimal performance for particle swarm 1. PMSM is a synchronous motor. Its main feature is that permanent magnet materials are installed on the rotor to generate a magnetic field, replacing the electromagnets in traditional synchronous motors [15]. In the PMSM, the magnetic field of the rotor rotates with mechanical rotation, while the stator is powered by an alternating-current power source to generate a rotating magnetic field. When these two magnetic fields are interlocked, the motor rotor will rotate synchronously with the stator magnetic field. Therefore, it is called the "synchronous motor". The physical model of PMSM is shown in Figure 2.

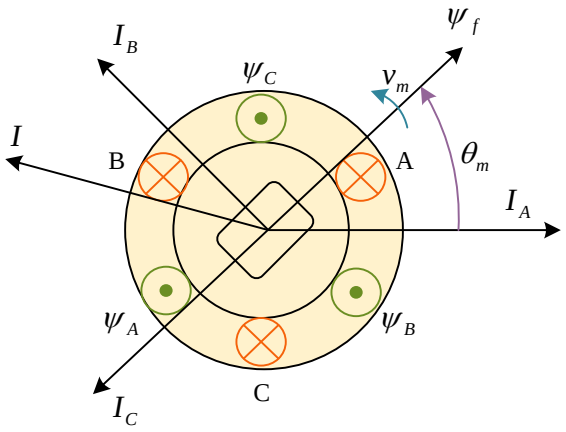

Figure 2: The physical model of PMSM

In Figure 2, in the physical model, A, B, and C respectively represent the stator windings of three-electrical phases. These windings are spaced 120 degrees apart in space and configured to generate three sinusoidal waveform currents with phase deviations of 120 degrees. When A, B, and C three-phase windings are fed with three-phase sinusoidal alternating-current, they generate magnetic fields in their respective phases [16]. Due to phase difference, these magnetic fields combine to form a rotating magnetic field that rotates at the same frequency as alternating current. This rotating magnetic field interacts with the permanent magnet on the rotor, causing the rotor to generate torque and rotate. The mathematical expression of PMSM stator winding magnetic flux is shown in equation (1).

$$\begin{bmatrix}\psi_A\\ \psi_B\\ \psi_C\end{bmatrix}=\begin{bmatrix}L_{AA} & M_{AB} & M_{AC}\\ M_{BA} & L_{BB} & M_{BC}\\ M_{CA} & M_{CB} & L_{CC}\end{bmatrix}\begin{bmatrix}I_A\\ I_B\\ I_C\end{bmatrix}+\begin{bmatrix}\psi_f\cos\theta\\ \psi_f\cos\left(\theta-\frac{2}{3}\pi\right)\\ \psi_f\cos\left(\theta+\frac{2}{3}\pi\right)\end{bmatrix} \quad (1)$$

In equation (1), ψ_A,ψ_B,ψ_C represent the magnetic flux of the stator windings A, B, and C. L,M represent the self-inductance coefficient and mutual inductance coefficient. I represents the current. ψ_f represents the magnetic flux generated by the permanent magnet itself. The voltage of the PMSM stator winding is shown in equation (2).

$$\begin{cases}U_A=RI_A+\dfrac{d\psi_A}{dt}\\ U_B=RI_B+\dfrac{d\psi_B}{dt}\\ U_C=RI_C+\dfrac{d\psi_C}{dt}\end{cases} \quad (2)$$

In equation (2), U_A,U_B,U_C represent the voltage of stator windings A, B, and C, respectively. R represents the resistance. The electromagnetic torque is shown in equation (3).

$$T_e=\frac{1}{2}P_n\times\frac{\partial\left(I_s\times\psi_s\right)}{\partial\theta_m} \quad (3)$$

In equation (3), T_e represents the electromagnetic torque. P_n represents the number of motor poles. ψ_s represents the magnetic flux vector. θ_m represents the mechanical angle. The mathematical expression for PMSM mechanical motion is shown in equation (4).

$$J\frac{dv_m}{dt}+\alpha v_m=T_e-T_L \quad (4)$$

In equation (4), J represents the rotational inertia. v_m signifies the mechanical angular velocity. T_L signifies the load torque. α represents the damping coefficient. The PMSM parameter identification model optimized by PSO is displayed in Figure 3.

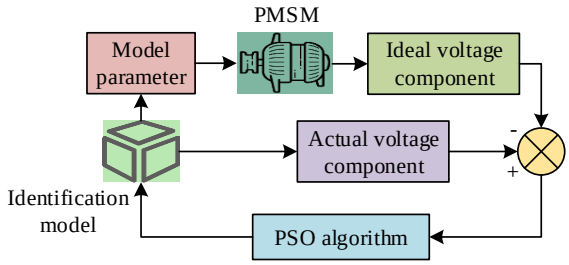

Figure 3: Design of PMSM parameter identification based on PSO optimization

In Figure 3, in the design of PMSM parameter identification model optimized by PSO, motor operating data, including voltage and current components, as well as back electromotive force, are first obtained under specific control conditions. These measurement values are input into the PSO algorithm to generate preliminary estimates. Then, the fitness function is defined by minimizing the sum of squares of the difference between the measured and estimated values. The PSO algorithm iteratively optimizes the fitness function, continuously updating the particle positions until it finds the parameter set that minimizes the fitness function. This set is the optimization identification result of the motor parameters [17]. The fitness function is displayed in equation (5).

$$f(x)=\sum_{t=1}^{n}\omega_1\left[U_d(t)-\hat{U}_d(t)\right]^2+\omega_2\left[U_q(t)-\hat{U}_q(t)\right]^2 \quad (5)$$

In equation (5), $f(x)$ represents the fitness function. ω_1 and ω_2 represent weight coefficients. U_d and U_q represent the stator voltage components on the direct and quadrature axes in the ideal motor model, respectively. $\hat{U}_d$ and $\hat{U}_q$ represent the stator voltage components on the direct and quadrature axes in the actual motor model, respectively.

3.2 Design of PMSM parameter system optimized by self-optimizing SA combined with PSO

The SA is a probabilistic optimization algorithm inspired by metal annealing in solid-state physics [18]. In metal annealing, the material is heated and then slowly cooled. Its internal structure becomes disordered at high temperature. As the temperature gradually decreases, the atoms gradually tend to become ordered, ultimately forming a stable crystal structure [19]. The combination of SA and PSO can fully utilize the advantages of both to form a hybrid optimization strategy, which uses SA to explore new possible solution spaces and avoid premature convergence, while PSO quickly refines after finding potential excellent solutions. This fusion method is expected to enhance the global search performance while maintaining fast convergence, thereby finding better solutions in various optimization problems. In the PSO algorithm, each particle iteratively updates its position and velocity in the search space, while the SA algorithm simulates the physical annealing process to find the global optimal solution to the optimization problem. Therefore, in the hybrid optimization algorithm formed by utilizing the global exploration ability of SA and the fast convergence characteristics of PSO, PSO algorithm can provide fast global search ability, and balance exploration and development by adjusting inertia weights and learning factors. The SA algorithm can enhance global search capability, avoid premature convergence, and explore a more optimal solution space by dynamically adjusting temperature and acceptance probability. Introducing greedy algorithms and memory tempering mechanisms into self optimization strategies can further optimize local search capabilities and prevent falling into local optima. The final hybrid optimization strategy can utilize the fast convergence of PSO and the global exploratory nature of SA to form a multi-level optimization process, improving the overall optimization ability and accuracy. The cohesive hybrid model based on SA and PSO integration is shown in Figure 4.

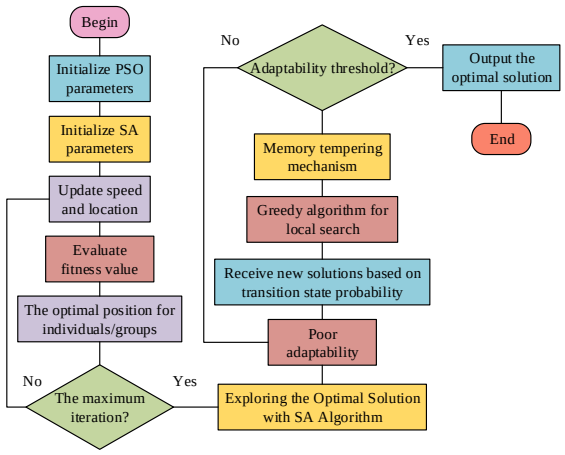

Figure 4: Cohesive hybrid model process based on SA and PSO integration

From Figure 4, in the cohesive mixing model based on SA and PSO, the PSO population is first initialized, including parameters such as particle position and velocity. The initial temperature and temperature decay coefficient of SA are set. Next, based on the velocity and position update formula of PSO, the position and velocity of particles are updated. The fitness value of each particle is evaluated, and the individual optimal position and group optimal position of the particles are updated. After each PSO iteration, the SA algorithm is used to explore the current optimal solution, calculate the fitness difference between the current solution and the new solution, and decide whether to accept the new solution based on the state transition probability of SA. Then, the temperature is updated and gradually lowered to reduce the possibility of accepting inferior solutions. During each iteration of the algorithm, the greedy algorithm is used to locally search for the current solution in order to refine the optimal solution. Finally, a memory tempering mechanism is introduced to record and trace back to the previous optimal solution, preventing falling into local optima. A fitness threshold is set. When the conditions are met, the algorithm terminates and outputs the optimal solution. The framework of PMSM parameter system based on SA-PSO is shown in Figure 5.

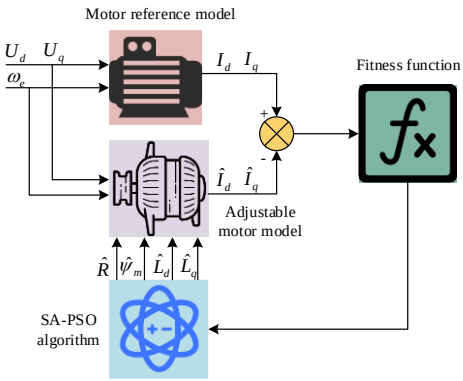

Figure 5: A PMSM parameter system framework based on SA-PSO

In Figure 5, in the PMSM parameter system framework ground on the SA-PSO, the voltage and current signals of the motor are treated as inputs to supply the

adjustable model and reference model of the motor. The difference in output current between these two models is used as an evaluation fitness function, which is the core indicator of algorithm optimization. The SA-PSO is committed to selecting more accurate parameters to be identified, with the goal of reducing the output bias in the adjustable benchmark model, and making the fitness function close to zero. The decrease in fitness value represents an improvement in identification accuracy. At present, motor parameter identification is achieved by storing the collected data and running the algorithm offline. To obtain PMSM parameters in real-time, the termination condition is set to synchronize with the system running time. It achieves continuous identification of each sampling point through a reset mechanism every 50 iterations, meeting online identification requirements. In this way, by collecting real-time direct-current/alternating-current axis voltage, current, and speed signals, motor parameters can be iteratively updated in real-time to adapt to dynamic working conditions. The core idea of PMSM parameter identification ground on SA-PSO is to minimize the error between the reference model output and the adjustable model output of the motor. The adjustable model is displayed in equation (6).

$$\frac{d}{dt}\begin{bmatrix}\hat{I}_d\\ \hat{I}_q\end{bmatrix}=\begin{bmatrix}-\frac{R}{L_d} & \frac{\omega_e L_q}{L_d}\\ -\frac{\omega_e L_d}{L_q} & -\frac{\hat{R}}{L_q}\end{bmatrix}\begin{bmatrix}I_d\\ I_q\end{bmatrix}+\begin{bmatrix}\frac{1}{\hat{L}_d} & 0\\ 0 & \frac{1}{\hat{L}_d}\end{bmatrix}\begin{bmatrix}U_d\\ U_q\end{bmatrix}+\begin{bmatrix}0\\ -\frac{\omega_e\hat{\psi}_m}{\hat{L}_q}\end{bmatrix} \quad (6)$$

In equation (6), ω_e signifies the electrical angular velocity. L_d, L_q signify the stator inductance on the direct and quadrature axes in the ideal model. $\hat{I}_d$ and $\hat{I}_q$ represent the output current current at the stator side on the direct and quadrature axes in the actual model, respectively. $\hat{\psi}_m$ represents the permanent magnet flux [20]. In motor parameter identification, to measure the similarity between the motor reference and the adjustable model, a suitable fitness function is designed. The fitness function defined is as follows.

$$\begin{cases} f_1\left(L_d, L_q, R\right)=\frac{1}{K}\left[I_d(k)-\hat{I}_d(k)\right]^2\\ f_2\left(L_d, L_q, R, \psi_m\right)=\frac{1}{K}\left[I_q(k)-\hat{I}_q(k)\right]^2\end{cases} \quad (7)$$

In equation (7), k signifies the number of iterations. K signifies the maximum number of iterations. f_1 signifies a fitness function that focuses on outputting response differences. The identifiable parameters are $\left(L_d, L_q, R\right)$. f_2 represents a fitness function that considers the dynamic behavior of the model, which can identify all parameters. The expression for updating parameter values is shown in equation (8).

$$\hat{R}(k)=\omega\hat{R}(k-1)+c_1\left[\hat{R}_{pbest}-\hat{R}(k-1)\right]+c_2\left[\hat{R}_{gbest}-\hat{R}(k-1)\right] \quad (8)$$

In equation (8), R_{pbest} and R_{gbest} respectively represent the optimal resistance of individuals and groups. The general expression for annealing is shown in equation (9).

$$T_{now}=\chi_1 T_1 \quad (9)$$

In equation (9), T_{now} represents the current temperature. χ_1 represents the initial temperature. T_1 represents the general annealing coefficient. The mathematical expression for rapid annealing is shown in equation (10).

$$T_{now}=\begin{cases} T_{now} & ,e^{\frac{-\Delta f}{T_{now}}<random(0,1)}\\ T_{now}+\chi_2^d T_2 & ,e^{\frac{-\Delta f}{T_{now}}>random(0,1)}\end{cases} \quad (10)$$

In equation (10), χ_2 represents the rapid annealing coefficient. d represents the number of times that the difference is received. T_2 represents the temperature at which tempering increases. $\Delta f=f_k-f_{k-1}$ represents the fitness deviation. If all parameters are represented by P, then the mathematical expression for the parameters after annealing according to equation (10) is shown in equation (11).

$$P=\begin{cases}1 & ,\Delta f\le 0\\ e^{\frac{-\Delta f}{T_{now}}} & ,\Delta f>0\end{cases} \quad (11)$$

To overcome the insufficient accuracy of PSO in handling multivariate parameter identification problems, as well as the insufficient rank of equation systems and the need for multiple experiments to determine fast annealing parameter settings in SA-PSO, a self-optimizing SA-PSO algorithm is proposed. This algorithm designs an innovative self-optimizing strategy by incorporating greedy optimization strategy and memory tempering mechanism into the PSO framework. In this strategy, PSO is endowed with the ability to accept inferior solutions with a certain probability, which significantly enhances the algorithm's ability to explore potential better solution spaces. At the same time, when the algorithm fails to evolve further after multiple iterations, greedy algorithms are used for local search to finely optimize the current solution, thereby solving the search space limitation that PSO may encounter in the later optimization process. The process of self-optimizing SA-PSO is shown in Figure 6.

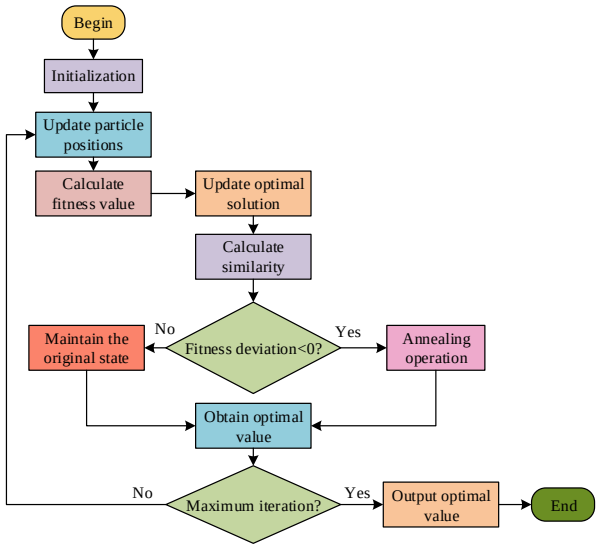

Figure 6: The process of self-optimizing SA-PSO

In Figure 6, in the self-optimizing SA-PSO, the particle position is first initialized, followed by fitness evaluation to update the optimal particle position and record the current optimal fitness parameters. If the fitness improvement brought by the new location is improved, it is migrated to the new location, and annealing operation is performed. Otherwise, it maintains the status quo. Through this process, the optimal state of individuals and groups is continuously optimized and recorded. Finally, if the predetermined iteration limit is realized, it returns the optimal solution. Conversely, the loop continues. The parameter update expression of the self-optimizing SA-PSO is shown in equation (12).

$$\hat{P}(k)=\omega\hat{P}(k-1)+c_1\left[\hat{P}_{pbest}-\hat{P}(k-1)\right]+c_2\left[\hat{P}_{gbest}-\hat{P}(k-1)\right] \quad (12)$$

In equation (12), $\hat{P}_{pbest}$ and $\hat{P}_{gbest}$ respectively represent the optimal parameters for individuals and populations. The inverse parameter is shown in equation (13).

$$\hat{P}'(k)=\omega'\hat{P}(k-1)+c_1\left[\hat{P}_{pbest}-\hat{P}(k-1)\right]+c_2\left[\hat{P}_{gbest}-\hat{P}(k-1)\right] \quad (13)$$

In equation (13), $\hat{P}'$ represents the inverse parameter. ω' represents the inverse inertia weight. The expression for fitness deviation is shown in equation (14).

$$\Delta f = f\left(\hat{P}(k)\right)-f\left(\hat{P}(k-1)\right) \quad (14)$$

The mathematical expression of the parameters after self-optimizing annealing is shown in equation (15).

$$P=\begin{cases}1, & \Delta f<0\\ e^{\frac{-0.001}{T_{now}}}, & \Delta f=0\\ e^{\frac{-\Delta f}{T_{now}}}, & \Delta f>0\end{cases} \quad (15)$$

After annealing according to equation (15), a refined search is conducted to obtain the optimal parameters.

4 Verification of PMSM parameter hybrid optimization strategy based on self-optimizing SA algorithm and PSO algorithm

This chapter first sets the parameters of PMSM and verifies the adaptive SA-PSO algorithm. Subsequently, the performance of the hybrid optimization strategy for PMSM parameters is validated in practical applications.

4.1 PMSM parameter setting and self-optimizing SA-PSO algorithm validation

Based on relevant data from a certain power grid company, simulation experiments of PMSM are conducted using MATLAB software. In the experiment, the maximum iterations are limited to 150. The learning factors $c1$ and $c2$ are fixed to 2. The learning rate is 0.5, and the inertia weight is 0.2867. The MATLAB software used is MATLAB R2023a version, and Simulink is used as a tool. The experimental hardware configuration uses an Intel Core i7 CPU, with an operating system configuration of Windows 10 and 16GB of RAM. The initial particle position is randomly distributed in the parameter space, and the initial particle velocity is set to 0. The parameter range of stator winding resistance is 1Ω to 4Ω. The parameter range of direct axis inductance and quadrature axis inductance is set from 5mH to 7mH. The parameter range of permanent magnet flux is set from 0.1Wb to 0.2Wb.

Initial parameters such as inertia weights, learning factors, and annealing coefficients in the research needs to consider the characteristics of the model. The selection should be based on the principle of ensuring steady-state tracking and filtering without divergence. The range of inertia weights selected is [0.1, 0.9], the learning factor is [1.5, 2.5], and the annealing coefficients is [0.80, 0.99]. To ensure coverage of the entire parameter space, the study sets the parameters of the above three coefficients as 5 sets of parameter ratios for parameter sensitivity analysis. The parameter sensitivity analysis results showed that the parameter combination with initial parameters such as inertia weight, learning factor, and annealing coefficient of 0.4, 2.0, and 0.95, respectively, had fast convergence speed, small final error, and high stability. Therefore, exploring this parameter combination for initial parameter setting can help improve the robustness of the method. The specific PMSM simulation parameters are displayed in Table 2.

Table 2: Specific PMSM simulation parameters

PMSM parameters	Values	PMSM Parameters	Values
Voltage/V	220	d-axis Inductance/mH	6.42
Current/A	4.2	q-axis Inductance/mH	6.42

Power/W	750	Permanent magnet flux chain/Wb	0.175
Stator winding resistance/Ω	2.875	Frequency/Hz	50
Rated speed/r▪min^{-1}	1000	Stator resistance/Ω	2.87

To evaluate the performance of the self-optimizing SA-PSO, simulation comparisons are conducted with PSO, SA, and traditional SA-PSO. The identification curves of the stator winding inductance on the direct and quadrature axes are shown in Figure 7. From Figure 7 (a), the self-optimizing SA-PSO on the direct axis stator winding showed an extremely fast convergence speed, approaching the preset inductance value only in the first 5 iterations. The inductance value obtained by the self-optimizing SA-PSO was 6.46mH. Compared with the ideal inductance value of 6.42mH, the error was only 0.62%. The identification errors of the standard PSO, SA, and SA-PSO were 1.40%, 1.09%, and 0.93%, respectively. From Figure 7 (b), the inductance value obtained by the self-optimizing SA-PSO on the quadrature axis stator winding was 6.44mH, with an error of 0.31%. The identification errors of the standard PSO, SA, and SA-PSO were 1.09%, 1.24%, and 0.77%, respectively. Overall, the self-optimizing SA-PSO has high identification accuracy.

The resistance and magnetic flux identification curves are displayed in Figure 8. In Figure 8 (a), the measured stator resistance value was 2.87 Ω. After the self-optimizing SA-PSO convergence, the resistance value obtained was 2.88 Ω, with an error of only 0.34%. In contrast, the identification errors of the standard PSO, SA, and SA-PSO were as high as 3.13%, 2.43%, and 2.13%, respectively. From Figure 8 (b), the actual magnetic flux value of the permanent magnet was 0.175Wb. The magnetic flux value identified by the self-optimizing SA-PSO was 0.184Wb, with an error of 5.14%. The errors of standard PSO, SA, and SA-PSO were 19.42%, 17.14%, and 14.28%, respectively. Overall, the self-optimizing SA-PSO algorithm shows high accuracy in identifying resistance and permanent magnet flux, which is significantly better than other comparative algorithms. This further confirms its effectiveness and superiority as a parameter identification tool. To further verify the reliability and stability of these error rates, the confidence intervals of error rates for each algorithm were calculated in multiple experiments. For resistance value identification, the error rate confidence interval of the self-optimizing SA-PSO algorithm was [0.31%,0.37%], indicating that the algorithm still maintained high consistency under different experimental conditions. The confidence intervals for the error rates of standard PSO, SA, and SA-PSO algorithms were [2.80%,3.46%], [2.18%,2.68%], and [1.95%,2.31%], respectively, indicating greater volatility and instability. For the identification of permanent magnet magnetic flux, the error rate confidence interval of the self-optimizing SA-PSO algorithm was [4.85%,5.43%], demonstrating good stability. In contrast, the error rate confidence intervals of the standard PSO, SA, and SA-PSO algorithms were [18.30%,20.54%], [16.40%,17.88%], and [13.90%,14.66%], respectively. These data further indicate that the self-optimizing SA-PSO algorithm has smaller fluctuations and is more reliable in magnetic flux identification.

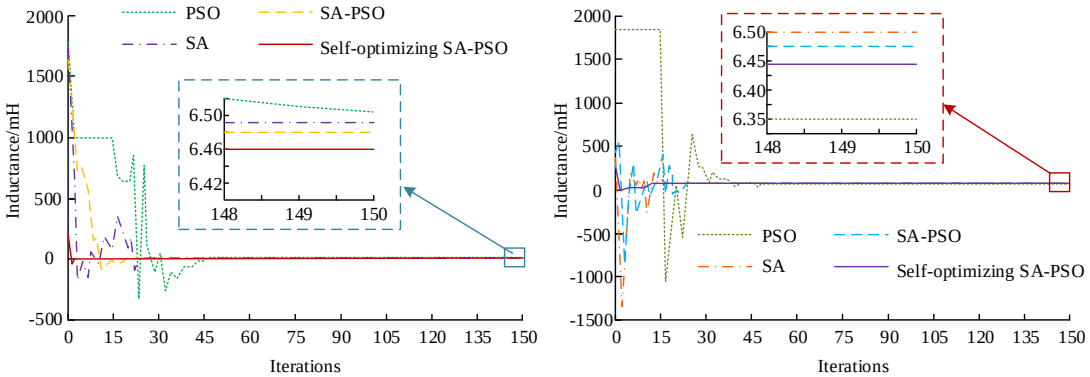

(a) Identification curve of direct axis stator winding inductance

(b) Identification curve of quadrature axis stator winding inductance

Figure 7. Identification curve of stator winding inductance for direct and quadrature axis

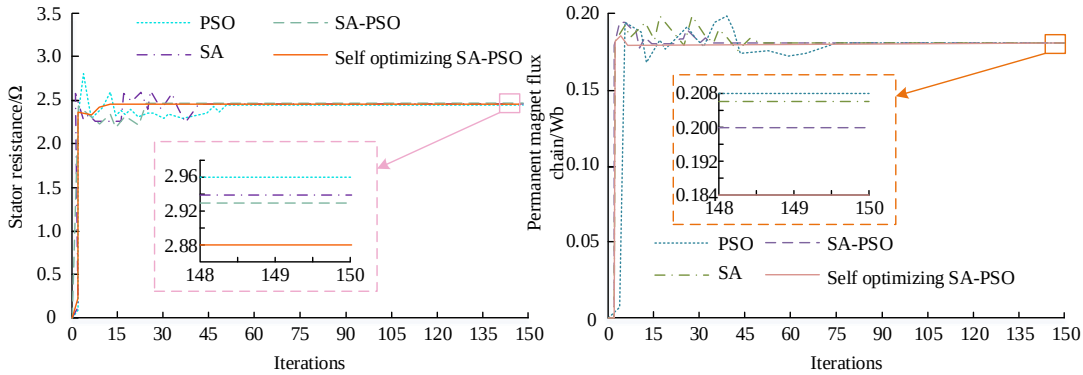

(a) The stator resistance curves of four algorithms

(b) Magnetic flux curves of permanent magnets using four algorithms

Figure 8: Identification curves of resistance and magnetic flux of permanent magnets using four algorithms

To further verify the effectiveness of the self-optimizing SA-PSO, 10 rounds of simulation experiments are conducted on these four algorithms. All the parameter identification data obtained are recorded. Table 3 displays the results. In Table 3, the difference between the maximum and minimum values of the self-optimizing SA-PSO was the smallest, with only 0.13 Ω. Compared with the other three algorithms, which were 0.51 Ω, 0.40 Ω, and 0.25 Ω, the difference reduced by 74.50%, 67.5%, and 23.52%, respectively. This significantly reduced difference indicates that the self-optimizing SA-PSO exhibits higher stability in resistance parameter identification. In terms of mean, the self-optimizing SA-PSO has neither the highest nor the lowest mean across various parameters, indicating that it may have achieved a balance in performance, with neither overestimation nor underestimation. These results indicate that the self-optimizing SA-PSO is a parameter identification tool that achieves a good balance between stability and accuracy.

Table 3: Parameter identification results of four algorithms

Algorithm		R/Ω	Ld/mH	Lq/mH	Permanent magnet flux chain/Wb
PSO	Maximum	2.97	6.94	6.81	0.232
	Minimum	2.46	6.23	6.33	0.188
	Average	2.65	6.61	6.52	0.207
SA	Maximum	2.95	6.89	6.77	0.225
	Minimum	2.55	6.33	6.35	0.200
	Average	2.89	6.54	6.56	0.208
SA-PSO	Maximum	2.97	6.80	6.87	0.222
	Minimum	2.72	6.36	6.34	0.197
	Average	2.80	6.51	6.50	0.202
Self-Optimizing SA-PSO	Maximum	2.89	6.79	6.78	0.202
	Minimum	2.76	6.41	6.38	0.180
	Average	2.82	6.46	6.47	0.189

4.2 Performance verification of PMSM parameter hybrid optimization strategy in practical applications

To verify the effectiveness of the PMSM parameter hybrid optimization strategy in practical applications, the set speed is suddenly changed from 2000rmp/min to 2500rmp/min at 0.1s. At 0.2s, the no-load is suddenly changed to a load of 5N·m. The changes in PMSM parameters over time are collected, as shown in Figure 9. From Figure 9 (a), within 0 to 0.1s, the three-phase currents of PMSM A, B, and C fluctuated between -10A and 10A. After 0.1s, the fluctuation range of the three-phase current was reduced to between -5A and 5A. This change is consistent with the set sudden change speed, proving the effectiveness of PMSM. From Figure 9 (b), after 0.1s, the angular velocity and rotational speed of PMSM also underwent a sudden change, with the rotational speed increasing from 2000rpm to 2500rpm and the angular velocity increasing from 800rad/s to 1000rad/s. These observation results are consistent with the experimental settings, indicating the effectiveness of the optimization strategy comprehensively.

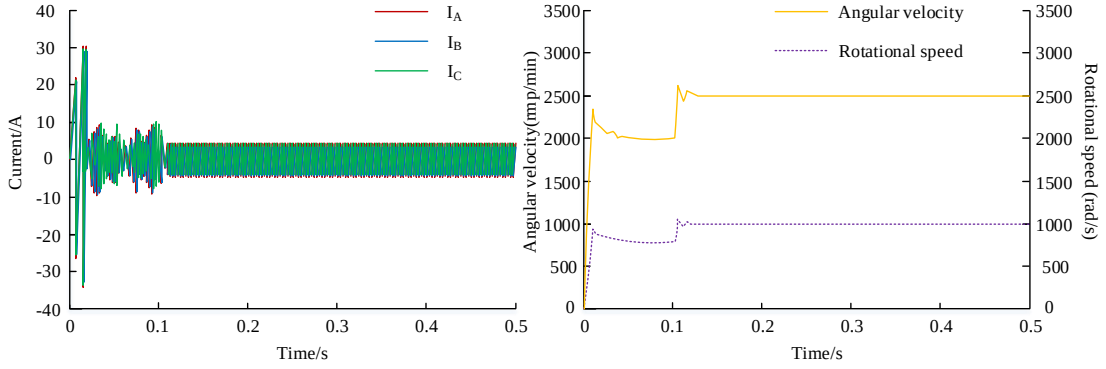

(a) The variation of three-phase current over time

(b) Changes in angular velocity and rotational speed over time

Figure 9: Changes in PMSM parameters over time

To further verify the stability of the strategy, the input current of the direct axis stator is 0. The changes in the current and voltage of PMSM on the direct and quadrature axes over time are monitored under these conditions, as shown in Figure 10. From Figure 10 (a), the direct axis stator was maintained at 0V, while the quadrature axis stator ultimately stabilized at 220V. The voltage of the entire system achieved rapid stability within 0.25s, indicating that the system had high response speed and excellent stability. From Figure 10 (b), the direct axis stator remained at 0A, while the quadrature axis stator stabilized at 5A. In the implemented optimization strategy, the PMSM exhibits good system stability with minimal voltage and current fluctuations.

To verify the actual performance of the self-optimizing SA-PSO in PMSM parameter adjustment, a comparison is made with PSO, SA, and traditional SA-PSO, as displayed in Table 4. From Table 4, the fitness of the hybrid strategy decreased by 70.83%, 52.98%, and 32.97% compared with PSO, SA, and traditional SA-PSO, respectively. The error rate of the hybrid strategy in identifying resistance, inductance, and magnetic flux was lower than the other three algorithms. This indicates that the hybrid strategy has advantages in the parameter identification accuracy. The identification speed of the hybrid optimization strategy was 0.114s, which was 28.30%, 24.50%, and 14.92% shorter than PSO, SA, and traditional SA-PSO, respectively. In summary, the self-optimizing SA-PSO exhibits accuracy and efficiency in PMSM parameter adjustment.

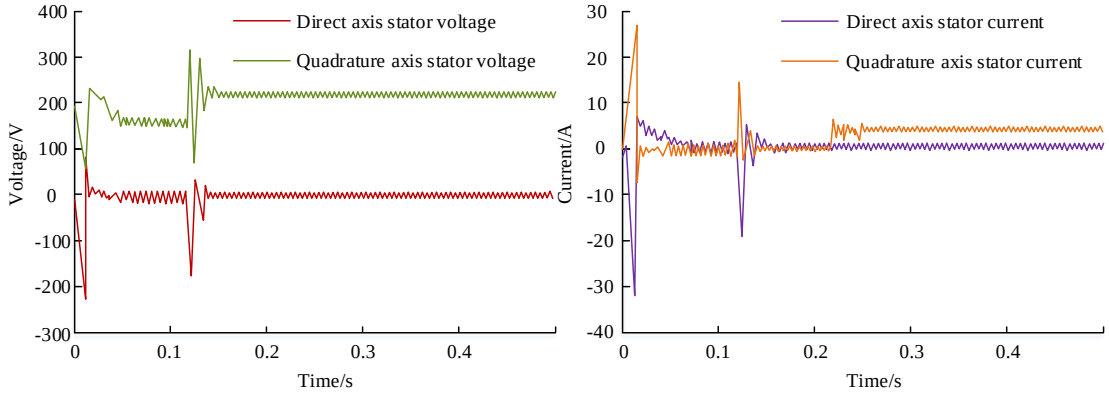

(a) The variation of stator voltage over time for both direct and cross axes

(b) The variation of stator current over time in both direct and quadrature axes

Figure 10: The variation of current and voltage over time on the straight and quadrature axes

Table 4: Average identification results of four optimization strategies

Parameter	Hybrid optimization strategy	PSO	SA	SA-PSO
Resistance/Ω	2.887	2.962	2.921	2.901
Error/%	0.46	3.77	2.31	1.79
Inductance/mH	8.31	8.591	8.504	8.416
Error/%	0.51	1.49	1.37	0.96
Permanent Magnet Flux Chain/Wb	0.301	0.274	0.281	0.297
Error/%	0.34	2.04	1.48	1.51
Identification Time/s	0.114	0.159	0.151	0.134

Fitness Value	0.63	2.16	1.34	0.94

The comparison table of the runtime performance of PSO, SA, SA-PSO, and self-optimizing SA-PSO in various scenarios is shown in Table 5. From Table 5, it can be seen that self-optimizing SA-PSO exhibits lower errors and better stability in most scenarios, especially in optimizing parameters such as magnetic field and resistance. Compared with other algorithms, it has better accuracy and smaller standard deviation, demonstrating its advantages in practical applications.

Table 5: The comparison table of the runtime performance of PSO, SA, SA-PSO, and self-optimizing SA-PSO in various scenarios

Scene	Index	Self-optimizing SA-PSO	PSO	SA	SA-PSO
Direct axis stator inductance	Error	0.62%	1.40%	1.09%	0.93%
Quadrature axis stator inductance	Error	0.31%	1.09%	1.24%	0.77%
Stator resistance	Error	0.34%	3.13%	2.43%	2.13%
Permanent magnet magnetic flux	Error	5.14%	19.42%	17.14%	14.28%
Multiple rounds of simulation experiments	Maximum minimum value difference	0.13Ω	0.51Ω	0.40Ω	0.25Ω
	Standard deviation	0.04	0.19	0.14	0.10
	stability	0.012	0.045	0.039	0.028

To further verify the robustness and wide applicability of the self-optimizing SA-PSO algorithm in PMSM parameter adjustment, its performance under transient conditions is analyzed, and the instantaneous increase of 200 revolutions per minute in speed under dynamic conditions is investigated. The PMSM parameter identification results of each optimization strategy under transient conditions are shown in Table 6. From Table 6, the resistance error, inductance error, and permanent magnet flux error of the self-optimizing SA-PSO strategy were 1.92%, 1.41%, and 1.36%, respectively, all less than 2%, which was significantly better than the performance of other methods. In addition, the response time of the research method was only 0.021 seconds, which was 34.37%, 67.69%, and 25% shorter than PSO, SA, and traditional SA-PSO, respectively, under transient bar change conditions. From the above, it can be seen that the self-optimizing SA-PSO algorithm has high robustness and wide applicability in PMSM parameter adjustment.

Table 6: PMSM parameter identification results of various optimization strategies under transient conditions

Parameter	Self-optimizing SA-PSO	PSO	SA	SA-PSO
Resistance error/%	1.92	4.67	12.48	2.45
Inductance error/%	1.41	5.26	6.56	3.38
Magnetic flux error of permanent magnet/%	1.36	3.10	5.63	2.53
Response time/s	0.021	0.032	0.065	0.028

5 Discussion

In recent years, PMSM has been widely used in high-performance applications due to its excellent performance. To improve the operating efficiency of PMSM and reduce maintenance costs, a parameter optimization method combining self-optimizing SA algorithm and PSO was designed. The research results indicated that there were differences in the results between self-optimizing SA-PSO and standard PSO, SA, and traditional SA-PSO algorithms. The self-optimizing SA-PSO algorithm exhibited excellent accuracy and stability in parameter identification, mainly due to its unique adaptive adjustment mechanism and optimization strategy. This is because the self-optimizing SA-PSO algorithm can dynamically adjust the search strategy based on the quality of the current solution, thereby maintaining efficiency throughout the entire search process. In contrast, standard PSO and SA algorithms do not have this adaptive ability, so they are prone to getting stuck in

local optima when dealing with complex search spaces, resulting in significant identification errors. In addition, SA-PSO combines the global search capability of SA algorithm and the local search capability of PSO. The self-optimizing SA-PSO further enhances this combination. Through adaptive adjustment, it significantly improves the resistance to noise and disturbance, thus exhibiting higher stability and accuracy in multiple rounds of simulation experiments. The self-optimizing SA-PSO exhibits a very fast convergence speed in identifying the inductance values on the stator windings of the straight and orthogonal axes, quickly approaching the preset values. In contrast, standard PSO and SA algorithms have slower convergence speeds and are easily affected by initial parameter settings, resulting in larger identification errors. The self-optimizing SA-PSO algorithm can effectively avoid getting stuck in local optima by dynamically adjusting the search strategy. This robustness enables the algorithm to maintain a small fluctuation range under different experimental conditions, thereby demonstrating high consistency and stability in multiple rounds of experiments. Sun X et al. optimized PMSM by adjusting the permanent magnet structure, air gap length, and stator core geometry to reduce torque ripple by 24% [6]. This method focused on improving the stability of motors in specific applications. However, this article not only considers the adjustment of structural parameters in optimizing motor performance, but also combines the optimized control strategy, further improving the efficiency and reliability of motors in practical use. He C et al. proposed an analysis method based on finite element model, which enhanced the overload capacity of PMSM by selecting a lower torque angle, thereby improving the overall performance of the motor [7]. This method effectively improves the durability of the motor, especially suitable for high load applications. However, this article further considers the dynamic response of the motor and combines advanced control algorithms to optimize the performance of the motor in transient response, making the motor not only perform excellently in steady state, but also maintain high efficiency and stability during transient load changes. Therefore, the self-optimizing SA-PSO algorithm exhibits high stability, accuracy, fast convergence, and robustness in parameter identification, making it significantly advantageous in PMSM parameter optimization.

6 Conclusion

In the PMSM parameter optimization, more efficient and accurate parameter identification methods are constantly receiving attention. Especially, optimizing parameters is crucial for improving the performance and efficiency of electric motors. The study aims to improve the convergence speed and identification accuracy of PMSM parameters by combining self-optimizing SA and PSO to enhance the efficiency of power system work in power grid companies. The results showed that the self-optimizing SA-PSO exhibited faster convergence speed and higher accuracy than traditional algorithms in identifying the inductance values of stator winding. The inductance value of the direct axis stator winding only approached the set target within 5 iterations, with an error rate of 0.62%, significantly better than the standard PSO, SA, and SA-PSO. The performance on the quadrature axis stator winding was also similar, with an error rate of 0.31%. In the identification of resistance values, the error rate of the self-optimizing algorithm was 0.34%, which was much lower than other algorithms. For the identification of permanent magnet magnetic flux, although the error rate of the self-optimizing SA-PSO was 5.14%, it was still lower than the error rate of the other three algorithms. In summary, the research on optimizing PMSM parameter systems using self-optimizing SA combined with PSO has significantly improved the accuracy and speed of parameter identification. In addition, the research method has applicability in high-performance electric vehicles, industrial automation systems, and specific application scenarios that require precise motor control, providing support and reference for the application of power grid systems or specific high-performance control environments. However, despite the excellent performance of the self-optimizing SA-PSO algorithm in multiple aspects, there is still room for improvement in the error rate of permanent magnet flux identification. Future work can focus on further reducing the error rate of magnetic flux identification and exploring the generalization ability of the algorithm under different motor types and operating conditions.

References

[1] Kauffman, J. M. (2022). Particle Swarm Optimization Algorithm and Its Applications: A Systematic Review. Archives of Computational Methods in Engineering, 29(5), 2531–2561. https://doi.org/10.1007/s11831-021-09694-4

[2] FENG Q, Li Q, QUAN W & PEI, X. M. Overview of multiobjective particle swarm optimization algorithm. Chinese Journal of Engineering, 2021, 43(6): 745-753.

[3] Xia, X., Gui, L., Yu, F., Wu, H., Wei, B., Zhang, Y., & Zhan, Z.-H. (2020). Triple Archives Particle Swarm Optimization. IEEE Transactions on Systems, Man, and Cybernetics, 50(12), 4862–4875. https://doi.org/10.1109/TCYB.2019.2943928

[4] Nayak, J., Swapnarekha, H., Naik, B., Dhiman, G., & Vimal, S. (2022). 25 Years of Particle Swarm Optimization: Flourishing Voyage of Two Decades. Archives of Computational Methods in Engineering, 30(3), 1663–1725. https://doi.org/10.1007/s11831-022-09849-x

[5] A Dynamic Neighborhood-Based Switching Particle Swarm Optimization Algorithm. (2022). IEEE Transactions on Cybernetics, 52(9), 9290–9301. https://doi.org/10.1109/tcyb.2020.3029748

[6] Sun, X., Shi, Z., Lei, G., Guo, Y., & Zhu, J. (2019). Analysis and Design Optimization of a Permanent Magnet Synchronous Motor for a Campus Patrol Electric Vehicle. IEEE Transactions on Vehicular Technology, 68(11), 10535–10544. https://doi.org/10.1109/TVT.2019.2939794

[7] He, C., & Wu, T. X. (2019). Analysis and design of surface permanent magnet synchronous motor and generator. 3(1), 94–100. https://doi.org/10.30941/CESTEMS.2019.00013

[8] Palangar, M. F., Soong, W. L., Bianchi, N., & Wang, R.-J. (2021). Design and Optimization Techniques in Performance Improvement of Line-Start Permanent Magnet Synchronous Motors: A Review. IEEE Transactions on Magnetics, 57(9), 1–14. https://doi.org/10.1109/tmag.2021.3098392

[9] Rafat Zaman, H. R., & Soleimanian Gharehchopogh, F. (2021). An improved particle swarm optimization with backtracking search optimization algorithm for solving continuous optimization problems. Engineering With Computers, 1–35. https://doi.org/10.1007/S00366-021-01431-6

[10] Liu, W., Wang, Z., Yuan, Y., Zeng, N., Hone, K., & Liu, X. (2021). A Novel Sigmoid-Function-Based Adaptive Weighted Particle Swarm Optimizer. IEEE Transactions on Systems, Man, and Cybernetics, 51(2), 1085–1093. https://doi.org/10.1109/TCYB.2019.2925015

[11] Position-Transitional Particle Swarm Optimization-Incorporated Latent Factor Analysis. (2022). IEEE Transactions on Knowledge and Data Engineering, 34(8), 3958–3970. https://doi.org/10.1109/tkde.2020.3033324

[12] He, F., & Ye, Q. (2022). A Bearing Fault Diagnosis Method Based on Wavelet Packet Transform and Convolutional Neural Network Optimized by Simulated Annealing Algorithm. Sensors, 22(4), 1410. https://doi.org/10.3390/s22041410

[13] Lee, S., & Kim, S. B. (2020). Parallel Simulated Annealing with a Greedy Algorithm for Bayesian Network Structure Learning. IEEE Transactions on Knowledge and Data Engineering, 32(6), 1157–1166. https://doi.org/10.1109/tkde.2019.2899096

[14] Alkhateeb, F., & Abed-alguni, B. H. (2019). A Hybrid Cuckoo Search and Simulated Annealing Algorithm. Journal of Intelligent Systems, 28(4), 683–698. https://doi.org/10.1515/jisys-2017-0268

[15] Kurtuluş, E., Yıldız, A. R., Sait, S. M., & Bureerat, S. (2020). A novel hybrid Harris hawks-simulated annealing algorithm and RBF-based metamodel for design optimization of highway guardrails. Materials Testing, 62(3), 251–260. https://doi.org/10.3139/120.111478

[16] Onyezewe, A., Kana, A. F., Abdullahi, F. B., & Abdulsalami, A. O. (2021). An Enhanced Adaptive k-Nearest Neighbor Classifier Using Simulated Annealing. International Journal of Intelligent Systems and Applications, 13(1), 34–44. https://doi.org/10.5815/ijisa.2021.01.03

[17] Chinthamu, N., & Karukuri, M. (2023). Data Science and Applications. Journal of Data Science and Intelligent Systems, 1(2), 83–91. https://doi.org/10.47852/bonviewjdsis3202837

[18] Chen, Y., Liang, S., Li, W., Liang, H., & Wang, C. (2019). Faults and Diagnosis Methods of Permanent Magnet Synchronous Motors: A Review. Applied Sciences, 9(10), 2116. https://doi.org/10.3390/app9102116

[19] Aryavalli, S. N. G., & Kumar, G. H. (2023). Futuristic Vigilance: Empowering Chipko Movement with Cyber-Savvy IoT to Safeguard Forests. Archives of Advanced Engineering Science, 2(4), 215–223. https://doi.org/10.47852/bonviewaaes32021480

[20] Han, L. H. N., Hien, N. L. H., Huy, L. V., & Hieu, N. V. (2024). A Deep Learning Model for Multi-Domain MRI Synthesis Using Generative Adversarial Networks. Informatica, 283–309. https://doi.org/10.15388/24-infor556